Inorganica Chimica Acta, 84 (1984) 221–227

Synthesis and Crystal and Molecular Structure of a Methyl N,N-Diethylcarbamylmethylenephosphonato Dysprosium Thiocyanate Complex

S. M. BOWEN, E. N. DUESLER and R. T. PAINE*

Department of Chemistry, University of New Mexico, Albuquerque, New Mex. 87131, U.S.A.

Received August 4, 1983

Bis-Methyl N,N-diethylcarbamylmethylenephosphonato dysprosium thiocyanate, $Dy[O_2P(OCH_3)CH_2C(O)N(C_2H_5)_2]_2(NCS)$ *was prepared from the combination of ethanolic solutions of* $Dy(NCS)_3 \cdot xH_2O$ *and* $(CH_3O)_2P(O)CH_2C(O)N(C_2H_5)_2$. *The complex was characterized by infrared and NMR spectroscopy, and single crystal X-ray diffraction methods. The crystal structure was determined at 25 °C from 3727 independent reflections by using a standard automated diffractometer. The complex was found to crystallize in the monoclinic space group* $P2_1/c$ *with* $a = 13.282(4)$ Å, $b = 19.168(5)$ Å, $c = 9.648(2)$ Å, $\beta = 90.09(2)°$, $Z = 4$, $V = 2456.4$ Å^3 *and* $\rho_{calcd} = 1.72$ g cm^{-3}. *The structure was solved by standard heavy atom techniques, and blocked least-squares refinement converged with* $R_F = 4.7\%$ *and* $R_{wF} = 4.9\%$. *The Dy atom is seven coordinate and bonded in a bidentate fashion to two anionic phosphonate ligands* $[O_2P(OCH_3)CH_2C(O)N(C_2H_5)_2^-]$ *through the carbonyl oxygen atoms and one of two phosphonate oxygen atoms. In addition, each Dy atom is coordinated to two phosphonate oxygen atoms from two neighboring complexes and to the nitrogen atom of a thiocyanate ion. This coordination scheme gives rise to a two-dimensional polymeric structure. Some important bond distances include Dy–NCS 2.433(8) Å, Dy–O(carbonyl)*$_{avg}$ *2.39(2) Å, Dy–O(equat. phosphoryl)*$_{avg}$ *2.303(8) Å, Dy–O(axial phosphoryl)*$_{avg}$ *2.25(2), P–O(phosphoryl)*$_{avg}$ *1.493(3) Å and C–O(carbonyl)*$_{avg}$ *1.25(1) Å.*

Introduction

Thiocyanate has been used in liquid–liquid extraction schemes for trivalent lanthanide and actinide ions, and some success has been achieved in effecting Am(III) and Ln(III) group separations in quaternary ammonium thiocyanate media [1, 2]. Surprisingly, little is known about the stoichiometry and structures of these particular complexes. A few attempts have been made to establish the stoichiometry of actinide and lanthanide thiocyanate extraction complexes containing neutral monofunctional phosphonates [3–7]. In particular, it has been propsed that a complex $Am(NCS)_3(TBP)_4$ forms in hexane solutions containing tri-butyl phosphate while Eu(III) forms a mixture of complexes, $Eu(NCS)_3(TBP)_3$ and $Eu(NCS)_3(TBP)_4$ [5, 6]. Another study indicated that in thiocyanate media, early lanthanides extract in a form $Ln(NCS)_3(R_3PO)_4$ and later lanthanides extract as $Ln(NCS)_3(R_3PO)_3$ [7].

Trivalent actinide and light lanthanide ions also are extracted from nitric acid and aqueous nitrate solutions by bifunctional carbamylmethylenephosphonates [8–11]; however, the effect of other counterions on these extractions has not been examined in detail until recently. Horwitz and coworkers [12] examined the influence of thiocyanate on the extraction of Am(III) and Eu(III) by dihexyl-N,N-diethylcarbamylmethylenephosphonate (DHDECMP), and based upon extraction data, they concluded that complexes of the type $Am(NCS)_3(DHDECMP)_4$ and $Eu(NCS)_3(DHDECMP)_4$ form in the organic phase. Further, they proposed that DHDECMP acts, as a bidentate ligand. This proposal difffers from earlier coordination models proposed by Horwitz for nitrate complexes in which it was assumed that tris, monodentate CMP complexes form with Am(III) and Ln(III) ions [11].

As part of our efforts to characterize the solution and solid state structures of liquid–liquid extraction complexes [13–17], we have studied the interactions of several carbamylmethylenephosphonate ligands with UO_2^{2+}, Th(IV) and a series of Ln(III) ions in thiocyanate solutions [18]. During the course of this study, it was observed that several CMP ligands, $(RO)_2P(O)CH_2C(O)NEt_2$ (R = Me, Et, i-Pr), undergo facile nucleophilic attack in the presence of KNCS, and anionic species $[(RO)P(O)_2CH_2C(O)NEt_2^-]$ were obtained in high yield [18]. The coordination chemistry of these anions has proven to be interesting, and we report here the synthesis, spectroscopic characterization and single crystal X-ray diffraction structure determination for the complex resulting from the combination of $Dy(NCS)_3$ and dimethyl-N,N-diethylcarbamylmethylenephosphonate (DMDECMP).

---

*Author to whom correspondence should be addressed.

0020-1693/84/$3.00

Experimental

General Information

The $(CH_3O)_2P(O)CH_2C(O)N(C_2H_5)_2$, (DMDECMP), was prepared by literature methods [19]. Dysprosium nitrate was obtained from Alpha Products and converted to $Dy(NCS)_3$ with KSCN [20]. Infrared spectra were recorded on a Nicolet Model 6000 FT-IR spectrometer by using KBr pellets. NMR spectra were recorded on a Varian FT-80 spectrometer operated at 32.2 MHz (^{31}P), 20.0 MHz (^{13}C) and 80.0 MHz (^{1}H). Samples were contained in 5mm tubes with a deuterated lock solvent. Spectral standards were 85% H_3PO_4(^{31}P) and $(CH_3)_4Si$(^{1}H, ^{13}C).

Preparation of the Complex

Typically, ethanolic solutions containing 27 mmol of $Dy(NCS)_3$ and 82 mmol of DMDECMP were combined, and a white solid was obtained upon evaporation of the ethanol. The solid was washed with benzene, redissolved in water and recrystallized by slow evaporation of the aqueous solution. *Anal.* Calcd for $DySP_2O_8N_3C_{15}H_{30}$: C, 28.3; H, 4.8; O, 20.1; N, 6.6; P, 9.7; S, 5.0; Dy, 25.5. Found: C, 29.6; H, 5.5; O, 24.0; N, 6.0; P, 10.5; S, 2.3; Dy, 22.0%. Infrared spectrum (cm^{-1}) (KBr pellet): 2072 (ν_{CN}, m), 1609 and 1595 (ν_{CO}, s), 1197 (ν_{PO}, s), 1049 (ν_{POC}, s). NMR spectra (D_2O, 27 °C): $^{31}P\{^{1}H\}$, δ 126; ^{1}H, δ 7.6, 1.9, 0.9; $^{13}C\{^{1}H\}$, δ 110.6, 63.7, 16.7, 11.3, 4.8.

Crystal Structure Determination

Crystals of the complex formed large, thin plates, and the plate face was determined to be [100]. In order to minimize absorption effects, a small plate (0.34 mm × 0.21 mm × 0.03 mm) was selected, and the crystal was glued to a glass fiber. The crystal was centered on a Syntex P3/F automated diffractometer, and the determinations of the crystal class, orientation matrix, and unit cell dimensions were performed in a standard manner [21]. Data were collected at 27 °C in the $\theta - 2\theta$ scan mode by using Mo-K_α radiation, a scintillation counter, and pulse height analyzer. A summary of the data collection parameters appears in Table I. Collected data were consistent with the assignment of a monoclinic space group $P2_1/c$. The data were corrected for Lorentz and polarization effects, and the redundant and equivalent reflections were averaged and converted to unscaled $|F_o|$ values. Corrections for absorption were made empirically based upon ψ scans. A laminar absorption correction was employed in which three parameters (the value of μt and two edge effect factors) were refined to fit a thin plate of major face [100]. The merging R values before and after absorption correction on the ψ scans were 4.5% and 2.5%. The estimated minimum and maximum transmission factors were 0.990 and 0.632.

TABLE I. Experimental Data for the X-Ray Diffraction Study of $Dy[O_2P(OCH_3)CH_2C(O)N(C_2H_5)_2]_2(NCS)$.

Crystal system:	monoclinic
Space group:	$P2_1/c$
a Å	13.282(4)
b Å	19.168(5)
c Å	9.648(2)
β deg	90.09(2)
V Å^3	2456.4
Z	4
μ(MoK_α)	33.2 cm^{-1}
$F(000)$	1268
mol. wt.	636.91
ρ(calcd g cm^{-3})	1.72
ρ(expt g cm^{-3})	1.78
diffractometer	Syntex P3/F
radiation	MoK_α(λ = 0.71069 Å)
temperature	27 °C
monochromator	highly oriented graphite crystal
reflections measured	h, k, ±l
2θ range	1°–55°
scan type	$\theta - 2\theta$
scan speed	2.02–29.3°/min
scan range	from $[2\theta(K_{\alpha_1}) - 1.1]°$ to $[2\theta(K_{\alpha_1}) + 1.1]°$
bkgd measurement	stationary crystal counter; at beginning and end of 2θ scan time each for one-fourth the total 2θ scan time
std. reflections	3 measured every 96 reflection [700, 080, 004]; no significant changes in intensity were observed.
independent reflec. collected	5683
unique reflections used	3727 with $F \geqslant 8\sigma(F)$
number of parameters	248
goodness of fit, $[\Sigma w(\lvert F_o\rvert - \lvert F_c\rvert)^2/(m - n)]^{1/2}$	0.95
weighting scheme:	$1/[\sigma(F)^2 + gF_0^2]$, g = 0.0046

Solution and Refinement of the Structure

All calculations were performed on a R3/SHELXTL structure determination package [21]. Anomalous dispersion terms were included for atoms with $Z \geqslant 2$. Least-squares refinement in this package uses a blocked cascade algorithm with full-matrix blocks of 102 parameters [22]. The solution and early refinements of the structure were based upon 4163 reflections with $F \geqslant 5\sigma(F)$. With the small crystal volume and large μ (33.2 cm^{-1}) a large number of weak reflections are expected. To minimize this, the data were treated with a crude profile analysis procedure during the geometric correction process. Profile fitting would be expected to improve the precision of measurement for weak reflections. (The number of observed reflections at $5\sigma(F)$ is 4163 with profile fitting and 3670 without profile fitting.)

A Patterson map revealed the positions of the Dy atom and two P atoms. Difference Fourier maps obtained by phasing on the heavy atoms yielded positions for the remaining nonhydrogen atoms. Isotropic refinement of all nonhydrogen atoms converged with $R_F = 11.5\%$. Application of individual anisotropic thermal parameters to all nonhydrogen atoms resulted in an $R_F = 5.2\%$. Large anisotropic thermal parameters on N(2), C(10), C(11), C(12), and C(13) indicated disorder in these atom positions. A simple 'two site occupancy' model seemed appropriate from the difference maps and the occupancies of the major and minor sites converged at 54% and 46%. The minor N(2)–C(12)–C(13) arm of the disordered amide, upon further refinement, diverged from its initial position resulting in unreasonable C–C bond lenghts, 1.7–1.8 Å. These positions were, therefore, fixed as found in the initial difference map and not allowed to vary in the final cycles of refinement. All hydrogen atoms except those on the disordered group were included in the final refinement as fixed contributors with their positions calculated and their isotropic thermal parameters equal to 1.2 to 1.3 times the U_{iso} of their parent carbon atoms.

Examination of the $|F|_{calcd}$ *vs.* $|F|_{obs}$ values at the end of the least squares refinement revealed 15 reflections for which $|F|_{obs}$ differed substantially from $|F|_{calcd}$: all of these were high angle reflections oriented such that the maximum attenuation by absorption would take place. Eight of these would have been very weak or unobserved if not for the severe absorption correction. These eight reflections have $I \leqslant 8\sigma(F)$ even with the absorption correction. This threshold for observation was used in the final refinements and the structure factor tables contain only those reflections for which $I > 8\sigma(F)$. Final least squares refinements based upon 3727 reflections with $F \geqslant 8\sigma(F)$ gave $R_F = 4.7\%$ and $R_{wF} = 4.9\%$. A final difference map showed the first nine peaks (1.91–1.15 eÅ^3) to be ≤0.97 Å from the Dy atom or near the disordered amide atoms. The observed and calculated structure factor amplitudes (Table S-1) and hydrogen atom positional parameters are available. The nonhydrogen atom fractional coordinates and anisotropic thermal parameters are listed in Table II.

The validity of augmenting the data set with the peak profile analysis was tested as follows: another data set not using the profile analysis but having approximately the same number of observed reflections (3670 reflections $> 5\sigma(F)$) was refined with the model. The resulting agreement factor ($R_F = 4.9\%$) and standard deviations on the bond lengths and angles were higher, reflecting a poorer quality refinement. Consequently, all results reported here refer to the previously described data set augmented by the profile analysis.

Results and Discussion

As mentioned above, the reaction of KNCS and DMDECMP in neutral aqueous solution results in carbon–oxygen bond cleavage on the phosphonate group [18]. This chemistry is summarized by the following equation. Similarly, the reaction of

$$(CH_3O)_2P(O)CH_2C(O)N(C_2H_5)_2 + KNCS \xrightarrow{H_2O}$$

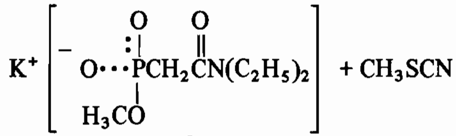

$$K^+\left[\begin{array}{c} \overset{O}{\underset{}{\vdots}}\;\;\overset{O}{\|} \\ {}^-O\cdots\underset{H_3CO}{\overset{|}{P}}CH_2CN(C_2H_5)_2 \end{array}\right] + CH_3SCN$$

1

DMDECMP with Dy(NCS)$_3$ in ethanol or water results in carbon–oxygen bond cleavage and the formation of a water and ethanol soluble complex, *2*. Satisfactory elemental analyses of *2* were difficult to obtain due to incomplete nucleophilic displacement; however, the analyses are most consistent with a complex containing a Dy(III) ion, one NCS ion and two anionic ligands, *1*. The chemistry responsible for the formation of *2* is, therefore, represented by the following equation.

$$(CH_3O)_2P(O)CH_2C(O)N(C_2H_5)_2 + Dy(NCS)_3 \cdot xH_2O \xrightarrow{EtOH}$$

$$\underset{2}{Dy[O_2P(OCH_3)CH_2C(O)N(C_2H_5)_2]_2(NCS)} + 2CH_3SCN + xH_2O$$

An infrared spectrum of *2* obtained from a KBr pellet displays a doublet at 1609 and 1595 cm^{-1} which can be assigned to ν_{CO} of one or more coordinated phosphonate ligand. Neutral DMDECMP shows a single carbonyl stretch at 1641 cm^{-1} and $K[O_2P(OCH_3)CH_2C(O)N(C_2H_5)_2]$ shows a related band at 1627 cm^{-1}. The down frequency shifts, $\Delta\nu_{CO} = -30$ cm^{-1} to -46 cm^{-1}, in *2* compared to neutral DMDECMP appear to be diagnostic of carbonyl oxygen atom coordination to Dy(III) [13–16, 19]. For example, $Th[(EtO)_2P(O)CH_2C(O)NEt_2]_2(NO_3)_4$ *3* [14], $Sm[(i\text{-}PrO)_2P(O)CH_2C(O)NEt_2]_2(NO_3)_3$ *4* [13] and $UO_2[(i\text{-}PrO)_2P(O)CH_2C(O)NEt_2](NO_3)_2$ *5* [15] show $\Delta\nu_{CO} = -51$, -31 to -55 and -41 cm^{-1}, respectively. Single crystal X-ray diffraction structure determinations for *3–5* confirm carbonyl oxygen–metal atom coordination. The $\Delta\nu_{CO}$ for $Er[(i\text{-}PrO)_2P(O)CH_2C(O)NEt_2]_2(NO_3)_3 \cdot H_2O$ *6* [13] was found to be smaller, -27 cm^{-1}, and the solid state structure contains carbonyl oxygen atoms bonded to the protons of a coordinated water molecule instead of the Er(III) atom.

TABLE II. Fractional Coordinates and Thermal Parameters (A × 10^3)[a] for $Dy[O_2P(OCH_3)CH_2C(O)N(C_2H_5)_2]_2(NCS)$.

Atom	x/a	y/b	z/c	U_{11}	U_{22}	U_{33}	U_{23}	U_{13}	U_{12}
Dy	0.07024(3)	0.37184(2)	0.35990(3)	37.0(2)	19.4(2)	23.8(2)	−2.3(1)	−3.4(1)	0.9(2)
P(1)	0.0530(2)	0.2015(1)	0.5063(2)	37(1)	27(1)	28(1)	5(1)	−1(1)	−1(1)
O(1)	0.0226(4)	0.2757(3)	0.4853(6)	44(3)	26(3)	35(3)	2(2)	4(3)	−2(2)
O(2)	−0.0266(5)	0.1498(4)	0.4436(7)	46(4)	43(3)	48(4)	4(3)	−6(3)	−14(3)
O(3)	0.0711(5)	0.1781(3)	0.6511(6)	67(5)	51(4)	34(3)	16(3)	−1(3)	4(3)
O(4)	0.2202(5)	0.3057(3)	0.3864(7)	41(3)	34(3)	56(4)	8(3)	5(3)	−1(3)
N(1)	0.3266(6)	0.2341(4)	0.4965(8)	41(4)	52(5)	50(5)	11(4)	−4(4)	2(4)
C(1)	0.2406(6)	0.2464(4)	0.4315(8)	37(4)	36(4)	33(4)	2(3)	4(3)	5(4)
C(2)	0.1688(6)	0.1886(4)	0.4056(10)	37(5)	29(4)	53(5)	−5(4)	8(4)	2(3)
C(3)	0.4011(9)	0.2919(7)	0.5048(12)	61(7)	90(9)	57(7)	11(6)	4(6)	−17(7)
C(4)	0.3816(14)	0.3348(11)	0.6305(16)	112(14)	153(17)	101(13)	−54(12)	−12(10)	−25(13)
C(5)	0.3501(9)	0.1684(7)	0.5706(11)	58(7)	92(9)	56(7)	39(6)	5(5)	−0(6)
C(6)	0.4095(12)	0.1186(7)	0.4867(17)	99(11)	80(9)	106(12)	28(8)	18(9)	48(9)
C(7)	−0.0739(9)	0.1614(6)	0.3135(10)	61(7)	69(7)	51(6)	−8(5)	−16(5)	−15(6)
P(2)	−0.0983(2)	0.5156(1)	0.3470(2)	45(1)	23(1)	25(1)	−2(1)	−9(1)	1(1)
O(5)	−0.0980(5)	0.5828(3)	0.4259(6)	66(4)	24(3)	29(3)	−3(2)	−11(3)	1(3)
O(6)	−0.1522(5)	0.5327(3)	0.2042(6)	64(4)	36(3)	28(3)	−8(2)	−14(3)	12(3)
O(7)	0.0007(4)	0.4807(3)	0.3211(6)	42(3)	24(3)	44(3)	7(2)	−6(3)	−1(2)
O(8)	−0.1082(5)	0.3546(3)	0.3301(8)	47(4)	28(3)	86(5)	−4(3)	−18(4)	−1(3)
C(8)	−0.1868(7)	0.3890(5)	0.3510(11)	32(4)	30(4)	76(7)	−2(4)	−14(4)	2(4)
C(9)	−0.1810(7)	0.4543(5)	0.4335(9)	45(5)	42(5)	40(5)	−8(4)	−5(4)	−1(4)
C(14)	−0.1304(9)	0.4944(5)	0.0780(9)	92(8)	54(6)	31(5)	−15(4)	−16(5)	15(6)
S(1)	0.3426(3)	0.5527(2)	0.2251(8)	73(2)	65(2)	100(3)	6(2)	13(2)	−29(2)
N(3)	0.2071(6)	0.4445(4)	0.2751(8)	52(5)	36(4)	43(4)	2(3)	5(4)	−3(4)
C(15)	0.2642(8)	0.4896(5)	0.2565(9)	56(6)	42(5)	36(5)	−1(4)	9(4)	4(4)
				U_{ISO}					
N(2)	−0.2673(18)	0.3745(11)	0.2691(25)	82(3)[b]					
N(2′)	−0.2795	0.3598	0.3336						
C(10)	−0.2579(20)	0.3151(14)	0.1377(27)						
C(10′)	−0.2757(24)	0.3084(17)	0.2068(32)						
C(11)	−0.3121(20)	0.2532(14)	0.1651(28)						
C(11′)	−0.3183(23)	0.2502(17)	0.2537(33)						
C(12)	−0.3588(20)	0.4206(14)	0.2621(28)						
C(12′)	−0.3753	0.3950	0.3519						
C(13)	−0.4276(19)	0.4186(15)	0.3439(26)						
C(13′)	−0.3932	0.4600	0.2373						

[a] The anisotropic temperature factor exponent takes the form: $-2\pi^2(h^2a^{*2}U_{11} + k^2b^{*2}U_{22} + \ldots + 2hka^*b^*U_{12} + \ldots)$. [b] A common U_{iso} was refined for the disordered NEt group.

The infrared spectrum of *2* also shows a strong band at 1197 cm^{-1} which is assigned to a phosphoryl group coordinated to the Dy(III) atom. This frequency compares with bands in the neutral ligand, 1260 cm^{-1}, and in *1*, 1235 cm^{-1} [18]. The shift, $\Delta\nu_{PO}$ = −73 cm^{-1}, from the neutral ligand compares well with coordination shifts found in the complexes listed above: *3* −70 cm^{-1} to −93 cm^{-1}; *4* −47 cm^{-1}; *5* −61 cm^{-1}, and *6* −46 cm^{-1}. The crystal structure for each of these complexes reveals metal–phosphoryl oxygen atom interactions. Thus, the infrared spectrum for *2* supports the existence of Dy–O=P and Dy–O=C interactions. The 'doublet' character of the carbonyl band has been observed in other metal–CMP complexes [13, 19]; however, a thorough understanding of this effect has not yet been obtained. The C–N stretch for the thiocyanate ion appears at 2072 cm^{-1} in *2*, and this compares with a range, 2076–2028 cm^{-1}, found in a number of lanthanide thiocyanate compounds [20, 23, 24].

Paramagnetic shifts and line broadening [25] dramatically effect the ^1H, $^{13}C\{^1H\}$ and $^{31}P\{^1H\}$ NMR spectra of *2* and little conclusive information pertaining to the solution structure can be presented. The $^{31}P\{^1H\}$ spectrum shows a broad singlet centered at 126 ppm which is approximately 102 ppm downfield of the resonance in DMDECMP. The ^{13}C NMR spectrum shows several resonances one of which can be tentatively assigned to the thiocyanate carbon atom (110.6 ppm). The remaining resonances cannot be unambiguously assigned at this time [26]. The ^1H NMR spectrum shows three broad resonances. The resonances centered at 0.9 and 1.9 ppm can probably be assigned to methyl protons. Confident assignments of the remaining spectral features must await more detailed studies.

Chemical observations suggest that DMDECMP undergoes $H_3C{-}OP$ bond cleavage in the presence of thiocyanate ion provided by $Dy(NCS)_3$, and that a coordination complex *2* forms which contains two anionic $O_2P(OCH_3)CH_2C(O)N(C_2H_5)_2^-$ ligands. The potentially unique character of the complex compared to complexes formed between neutral CMP ligands and lanthanide nitrates and the absence of structurally definitive spectroscopic data led us to determine the solid state structure of *2* by X-ray diffraction techniques. The X-ray diffraction analysis confirms the composition of *2* as $Dy[O_2P(OCH_3)CH_2C(O)N(C_2H_5)_2]_2(NCS)$. A view of the molecular unit is shown in Fig. 1 and a stereoview of the crystal packing is shown in Fig. 2. Selected interatomic bond distances and angles are summarized in Tables III and IV.

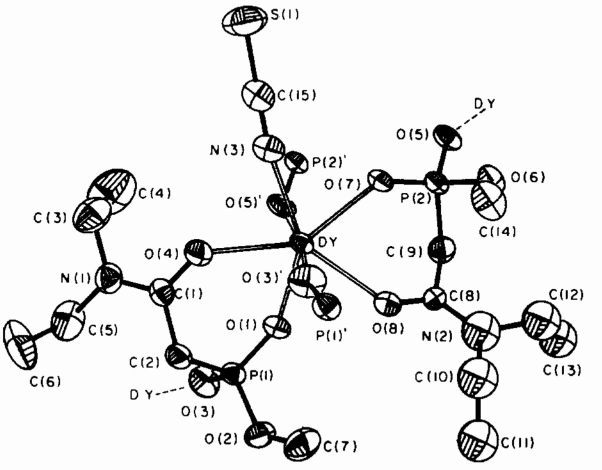

Fig. 1. Molecular geometry and atom labeling scheme for $Dy[O_2P(OCH_3)CH_2C(O)N(C_2H_5)_2]_2(NCS)$.

Each Dy(III) atom is bonded in a bidentate fashion to two anionic ligands, *1*. Coordination occurs with one of the two available phosphoryl oxygen atoms and the carbonyl oxygen atom on each ligand. In addition, each Dy(III) atom is bonded to the nitrogen atom of a thiocyanate ion and to two phosphoryl oxygen atoms from two neighboring units of *2*. The resulting structure is a two dimensional polymer which forms sheets perpendicular to the (100) direction. The seven atom coordination polyhedron is a pentagonal bipyramid in which the carbonyl and phosphoryl oxygen atoms of the bidentate chelate ring and the nitrogen atom of the NCS^- ion form the pentagonal belt. The two phosphoryl oxygen atoms from neighboring molecules are trans to each other, and they occupy the cap positions of the polyhedron. Seven coordinate lanthanide complexes are relatively rare [27]. For example, $Eu(C_{11}H_{19}O_2)_3 \cdot [(CH_3)_2SO]$ [28] forms a pentagonal bipyramid, $Eu(C_{11}H_{19}O_2)_3 \cdot (C_5H_{10}SO)$ [29] and $Ho(C_{15}H_{11}O_2)_3 \cdot H_2O$ [30] form capped octahedra and $Yb(C_5H_7O_2)_3 \cdot (C_5H_8ON)$ [31], $Yb(C_5H_7O_2)_3 \cdot H_2O$ [32] and $Dy(C_{11}H_{19}O_2)_3 \cdot H_2O$ [33] form capped trigonal prisms.

There are two groups of Dy–O (phosphonate) bonds in *2*: those comprising the pentagonal belt, $(Dy{-}O)_{avg}$ 2.303(8) Å and those involving the axial positions, $(Dy{-}O)_{avg}$ 2.25(2) Å [34]. The difference suggests that the Dy–O axial interactions may be slightly stronger than the Dy–O equatorial interactions. There appears to have been no previous crystallographic studies of Dy phosphonate complexes; therefore, direct bond distance comparisons are made difficult. The average metal–phosphoryl oxygen atom distances in our previously reported CMP complexes are *3 2.482* Å' *4* 2.418 Å, *5* 2.420 Å and *6* 2.259 and 2.290 Å. By taking into account differences in metal ionic radii [35] but neglecting differences in metal coordination numbers, it appears that the Dy–O axial and equatorial bond distances in *2* are slightly shorter than the metal–O distances in complexes which contain neutral CMP ligands.

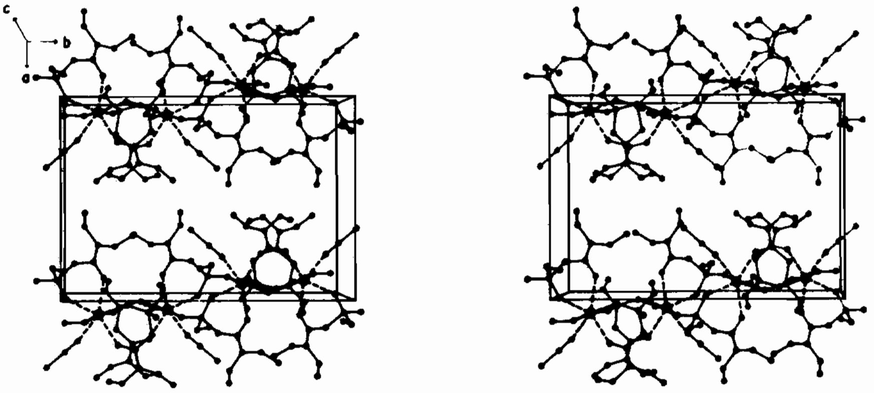

Fig. 2. Stereoview of the molecular packing for $Dy[O_2P(OCH_3)CH_2C(O)N(C_2H_5)_2]_2(NCS)$.

TABLE III. Selected Interatomic Bond Distances (Å) for $Dy[O_2P(OCH_3)CH_2C(O)N(C_2H_5)_2]_2(NCS)$.

Dy–N(3)	2.433(8)	Dy–O(3′)	2.230(6)
Dy–O(1)	2.295(5)	Dy–O(5′)	2.272(5)
Dy–O(4)	2.374(6)	N(3)–C(15)	1.164(12)
Dy–O(7)	2.311(5)	C(15)–S(1)	1.624(10)
Dy–O(8)	2.409(7)		
P(1)–C(2)	1.837(9)	P(2)–C(9)	1.813(9)
P(1)–O(1)	1.492(6)	P(2)–O(7)	1.496(6)
P(1)–O(2)	1.570(7)	P(2)–O(6)	1.586(6)
P(1)–O(3)	1.486(6)	P(2)–O(5)	1.497(6)
O(2)–C(7)	1.420(12)	O(6)–C(14)	1.451(11)
C(2)–C(1)	1.483(12)	C(9)–C(8)	1.484(13)
C(1)–O(4)	1.247(10)	C(8)–O(8)	1.252(11)
C(1)–N(1)	1.324(11)	C(8)–N(2)[a]	1.36(3)
C(3)–N(1)	1.488(15)	C(10)–N(2)[a]	1.64(3)
C(5)–N(1)	1.480(15)	C(12)–N(2)[a]	1.48(4)
C(3)–C(4)	1.487(21)	C(10)–C(11)[a]	1.37(4)
C(5)–C(6)	1.481(19)	C(12)–C(13)[a]	1.45(4)

[a] Average values for disordered atoms.

TABLE IV. Selected Interatomic Bond Angles (°) for $Dy[O_2P(OCH_3)CH_2C(O)N(C_2H_5)_2]_2(NCS)$.

O(1)–Dy–O(4)	75.3(2)	O(7)–Dy–O(8)	73.3(2)
O(1)–Dy–O(8)	71.4(2)	O(7)–Dy–N(3)	74.2(2)
O(1)–Dy–N(3)	147.6(2)	O(7)–Dy–O(1)	134.4(2)
O(1)–Dy–O(5′)	82.7(2)	O(7)–Dy–O(5′)	82.3(2)
O(1)–Dy–O(3′)	97.7(2)	O(7)–Dy–O(3′)	104.1(2)
O(3′)–Dy–O(5′)	170.0(2)	O(7)–Dy–O(4)	146.5(2)
Dy–O(1)–P(1)	139.7(3)	Dy–O(7)–P(2)	136.6(3)
Dy–O(4)–C(1)	134.9(6)	Dy–O(8)–C(8)	136.8(6)
Dy–O(3′)–P(1′)	167.8(4)	Dy–O(5′)–P(2′)	142.4(3)
O(1)–P(1)–O(2)	111.6(3)	O(7)–P(2)–O(6)	110.1(3)
O(1)–P(1)–O(3)	117.3(4)	O(7)–P(2)–O(5)	117.9(4)
O(2)–P(1)–O(3)	106.2(4)	O(5)–P(2)–O(6)	105.3(3)
O(1)–P(1)–C(2)	106.5(3)	O(7)–P(2)–C(9)	108.7(4)
O(2)–P(1)–C(2)	105.9(4)	O(6)–P(2)–C(9)	105.1(4)
O(3)–P(1)–C(2)	108.8(4)	O(5)–P(2)–C(9)	108.9(4)
O(4)–C(1)–C(2)	118.9(7)	O(8)–C(8)–C(9)	119.2(8)
N(1)–C(1)–O(4)	121.0(8)	N(2)–C(8)–O(8)[a]	119(1)
N(1)–C(1)–C(2)	120.0(8)	N(2)–C(8)–C(9)[a]	119(1)
P(1)–C(2)–C(1)	110.4(6)	P(2)–C(9)–C(8)	109.3(6)
Dy–N(3)–C(15)	164.6(7)		
N(3)–C(15)–S(1)	178.1(8)		

[a] Averaged values for disordered atoms.

The Dy–O(carbonyl)$_{avg}$ distance in *2*, 2.39(2) Å is slightly longer than the related Dy–O(carbonyl) distance in seven coordinate $Dy(thd)_3 \cdot H_2O$ [33, 36] 2.28 Å. The distance in *2*, on the other hand, is comparable to distances found in eight coordinate $Dy(NTA)(H_2O)_2 \cdot 2H_2O$ [36, 37] 2.35 Å and other metal–CMP complexes after corrections for ionic radii differences are considered: *3* (CN = 12) 2.453 Å, *4* (CN = 10) 2.433 Å and *5* (CN = 6 UO_2^{2+}) 2.406 Å. The Dy–N(3) bond distance, 2.433(8) Å, can be crudely compared to the Er–NCS bond distance in $Er[(C_4H_9)_4N]_3(NCS)_6$, 2.34(2) Å [38]. After radii corrections, the Dy–N distance is about 0.06 Å longer than the Er–N distance. These bond distance comparisons, however, must be treated carefully because of the widely differing coordination numbers involved.

Comparison of bond distances and angles in the coordinated CMP ligands in *3*–*5* with those of the anionic CMP ligands in *2* are also of interest. The four coordinated phosphoryl groups show an average P–O bond distance, 1.493(3) Å, which is slightly longer than the bond distances in *3* 1.478(4) Å, *4* 1.480(2) Å and *5* 1.485(5) Å. This trend is expected since the $P\overset{\cdot\cdot}{-}O$ multiple bond character in *1* and consequently *2* can be delocalized over two P–O bonds while multiple bonding in the neutral CMP ligands and their complexes is localized on one P=O group. The P–O(methyl) distances, 1.570(7) Å and 1.586(6) Å, are comparable to related distances in *3*–*5*. The carbonyl bond distances in *2*, 1.247(10) Å and 1.252(11) Å compare favorably with C=O distances in neutral CMP–metal nitrate complexes: *3* 1.256(6) Å, *4* 1.261(3) Å and *5* 1.260(8) Å. Lastly, inspection of the angles about the phosphorus atoms in *2* reveals that the phosphorus atom is tetrahedral and not dramatically distorted from the phosphorus atom geometry found in *3*–*5*.

The N-bonded thiocyanate group is nearly linear, N(3)–C(15)–S(1) 178.1(8)°, and the Dy–N(3)–C(15) vector is slightly bent, 164.6(7)°. The N(3)–C(15) bond distance, 1.164(12) Å, is short, while C(15)–S(1), 1.624(10) Å, is long. These distances are consistent with a resonance form $N{\equiv}C{-}S^-$ for the anion.

The chemical and structural results presented here provide two significant observations. Since thiocyanate is employed in conjunction with CMP extractants in selected lanthanide and actinide separations, care should be exercised in monitoring for CMP degradation which could result in unfavorable partitioning and extractant loss. At room temperature or slightly above, it appears that nucleophilic attack by NCS^- occurs only with $(RO)_2P(O)CH_2C(O)NEt_2$, R = Me, Et, i-Pr; however, it is not known whether the populary employed CMP extractants with R = Bu or Hx may undergo this reaction under strenuous radiolytic conditions. This chemistry is under study in our laboratory. In addition, the two dimensional polymeric structure adopted by *2* suggests that a new family of Ln and Ac layered phosphonate materials might be obtained from a synthetic procedure similar to that described here.

Acknowledgement

RTP wishes to recognize financial support for this research from the Department of Energy, Office of Basic Energy Sciences, Contract No. 79ER-10465. Grants from the NSF, CHE-7802921 and CHE-8007979 facilitated the purchase of the X-ray diffractometer and FT-IR spectrometer.

References

1 F. L. Moore, *Anal. Chem., 36*, 2158 (1964).

2 P. T. Gerontopolos, L. Rigali and P. G. Barbano, *Radiochem. Acta, 4*, 75 (1965).

3 T. Sekine and Y. Hasegawa, 'Solvent Extraction Chemistry', Marcel Dekker, Inc., N.Y. (1977) p. 523–566.

4 K. W. Bagnall, 'The Actinide Elements', Elsevier Publishing Co., N.Y. (1972).

5 W. F. Kinard and G. R. Choppin, *J. Inorg. Nucl. Chem., 36*, 1131 (1974).

6 T. Sekine, *Bull. Chem. Soc. Jpn., 38*, 1972 (1965).

7 P. K. Khopkar and P. J. Narayanankutty, *J. Inorg. Nucl. Chem., 34*, 2617 (1972).

8 W. W. Schulz and L. D. McIsaac, 'Transplutonium Elements', W. Müller and R. Lindner, Ed., North Holland, Amsterdam (1976).

9 L. D. McIsaac, J. D. Baker, J. F. Krupa, R. E. LaPointe, D. H. Meikrantz and N. C. Schroeder, Rept. ICP-1180, Allied Chemical Co., Idaho Chemical Programs, Idaho Falls, ID (1979).

10 L. D. McIsaac, J. D. Baker, J. F. Krupa, D. H. Meikrantz and N. C. Schroeder, 'Actinide Separations', *ACS Symposium Ser., 117*, 395 (1980).

11 E. P. Horwitz, A. C. Muscatello, D. G. Kalina and L. Kaplan, *Sep. Sci. Tech., 16*, 417 (1981).

12 A. C. Muscatello, E. P. Horwitz, D. G. Kalina and L. Kaplan, *Sep. Sci. Tech., 17*, 859(1982).

13 S. M. Bowen, E. N. Duesler and R. T. Paine, *Inorg. Chim. Acta, 61*, 155 (1982).

14 S. M. Bowen, E. N. Duesler and R. T. Paine, *Inorg. Chem., 21*, 261 (1982).

15 S. M. Bowen, E. N. Duesler and R. T. Paine, *Inorg. Chem., 22*, 286 (1983).

16 S. M. Bowen, E. N. Duesler, R. T. Paine and C. F. Campana, *Inorg. Chim. Acta, 59*, 53 (1982).

17 J. S. Jessup, E. N. Duesler and R. T. Paine, *Inorg. Chim. Acta, 73*, 261 (1983).

18 S. M. Bowen and R. T. Paine, to be published; S. M. Bowen, Ph.D. Thesis, University of New Mexico, Albuquerque, NM (1983).

19 T. H. Siddall, *J. Inorg. Nucl. Chem., 25*, 883 (1963); T. H. Siddall, *ibid., 26*, 1991 (1964).

20 D. R. Cousins and F. A. Hart, *J. Inorg. Nucl. Chem., 29*, 3009 (1967).

21 The P3/F and R3 hardware configuration has been described: C. F. Campana, D. F. Shepard and W. N. Litchman, *Inorg. Chem., 19*, 4039 (1981). Crystal centering, autoindexing, cell parameter refinement and axial photograph programs are those described in the 'Nicolet P3/R3 Operations Manual', Nicolet XRD Corp. 1980. All calculations and plots were performed with the SHELXTL-Revision 3. G. M. Sheldrick, 'Nicolet SHELXTL Operations', 1981. SHELXTL uses scattering factors compiled in 'International Tables for X-ray Crystallography', Vol. IV, Kynoch Press, Birmingham, U.K. (1968).

22 A general description of the least squares algebra is found in: 'Crystallographic Computing', F. R. Ahmed, S. R. Hall and C. P. Huber, Eds., Munksgaard Publ. Co., Copenhagen, p. 187 (1970).

23 G. Vicentini, R. Najjar, C. Airoldi, *An. Akad. Brasil Cienc., 41*, 375 (1969).

24 G. Vicentini, M. Perrier, L. B. Zinner, M. I. Amin, *J. Inorg. Nucl. Chem., 36*, 771 (1974).

25 A general discussion of paramagnetic line broadening by lanthanide ions appears in 'NMR of Paramagnetic Molecules, Principles, and Applications', G. N. LaMar, W. DeW. Horrocks and R. H. Holm, Eds., Academic Press, N.Y. 1973. Paramagnetic broadening in Dy(III) complexes is typically severe.

26 Full assignments of ^{1}H and ^{13}C NMR spectra for the corresponding La(III) complex have been completed, and this work will be reported separately [18].

27 D. K. Koppikar, P. V. Sivapullaiah, L. Ramakrishnan and S. Soundararajan, *Structure and Bonding, 34*, 135 (1978).

28 D. S. Dyer, J. A. Cunningham, J. J. Brooks and R. E. Sievers, 'Nuclear Magnetic Resonance Shift Reagents', R. E. Sievers, Ed., Academic Press, NY (1973) p. 33.

29 J. J. Uebel and R. M. Wing, *J. Am. Chem. Soc., 94*, 8910 (1972).

30 A. Zalkin, D. H. Templeton and D. G. Karraker, *Inorg. Chem., 8*, 2680 (1969).

31 M. F. Richardson, P. W. R. Corfield, D. E. Sands and R. E. Sievers, *Inorg. Chem., 9*, 1632 (1970).

32 J. A. Cunningham, D. E. Sands, W. E. Wagner and M. F. Richardson, *Inorg. Chem., 8*, 22 (1969).

33 C. S. Erasmus and J. C. A. Boeynes, *J. Cryst. Mol. Struct., 1*, 83 (1971).

34 The errors listed in (   ) for *averaged* distances were calculated by using the equation $(\sigma_l) = [\Sigma_m(lm - \bar{l})^2/m(m-1)]^{1/2}$ where $\bar{l}$ = avg. dist., l_m = individual dist. and m = number of distances.

35 R. D. Shanon and C. T. Prewitt, *Acta Crystallogr., B25*, 925 (1979). The effective ionic radii with coordination number eight were used for comparisons in the text: Th(IV) 1.06 Å, Sm(III) 1.09 Å, Eu(III) 1.07 Å, Dy(III) 1.03 Å, Ho(III) 1.02 Å, Er(III) 1.00 Å and Yb(III) 0.98 Å.

36 Abbreviations used in the text include (thd) = 2,2,6,6-tetramethyl-3,5-heptanedionate, (NTA) nitrilotriacetate.

37 L. L. Martin and R. A. Jacobson, *Inorg. Chem., 11*, 2789 (1972).

38 J. L. Martin, L. C. Thompson, L. J. Radonovich and M. D. Glick, *J. Am. Chem. Soc., 90*, 4494 (1968).